

See discussions, stats, and author profiles for this publication at: <https://www.researchgate.net/publication/27264273>

# Real-Time Observation of Intra- and Intermolecular Vibrational Energy Flow of Selectively Excited Alkyl Iodides in Solution: The Effect of Chemical Substitution

ARTICLE in THE JOURNAL OF PHYSICAL CHEMISTRY A · MAY 2002

Impact Factor: 2.69 · DOI: 10.1021/jp015552y · Source: OAI

---

CITATIONS

32

---

READS

11

6 AUTHORS, INCLUDING:



Klaus Luther

Georg-August-Universität Göttingen

117 PUBLICATIONS 1,975 CITATIONS

SEE PROFILE



Bernd Abel

Leibniz Institute of Surface Modification

137 PUBLICATIONS 1,956 CITATIONS

SEE PROFILE

## LETTERS

### Real-Time Observation of Intra- and Intermolecular Vibrational Energy Flow of Selectively Excited Alkyl Iodides in Solution: The Effect of Chemical Substitution

J. Assmann,<sup>†</sup> A. Charvat,<sup>†,‡</sup> D. Schwarzer,<sup>‡</sup> C. Kappel,<sup>†</sup> K. Luther,<sup>†</sup> and B. Abel<sup>\*,†</sup>

*Institut für Physikalische Chemie der Universität Göttingen, Tammannstrasse 6, 37077 Göttingen, Germany, and Max-Planck Institut für Biophysikalische Chemie, Am Fassberg, 37077 Göttingen, Germany*

*Received: October 4, 2001; In Final Form: February 18, 2002*

Intramolecular vibrational energy redistribution (IVR) and intermolecular vibrational energy transfer (VET) of two alkyl iodides ( $\text{CF}_3\text{CH}_2\text{I}$  and  $\text{CH}_3\text{CH}_2\text{I}$ ) selectively excited in the two quanta overtone region of the CH stretch vibration ( $\nu_{\text{CH}} = 2$ ) were measured in real time in solution. In this study, we have focused on the effect of chemical substitution on the mechanisms and time scales of IVR and VET of this family of molecules. With a simple model, we have obtained global IVR and VET rate coefficients for both molecules. The magnitude and the variation of the relaxation rates upon chemical substitution provide evidence for a survival of hierarchical IVR in these solvated molecules, which is governed by specific low-order intramolecular interactions and which can be rationalized with a simple low-order coupling model. At the same time, the general assumption that VET is simply dominated by the lowest-frequency modes in a molecule is not supported.

#### I. Introduction

Intramolecular vibrational energy redistribution (IVR) and intermolecular vibrational energy transfer (VET) are important for many reactive processes, as well as for a control of chemical dynamics in solution. It is well-known that both govern the rates, pathways, and efficiencies of chemical transformations. Despite their importance for the dynamics in the condensed phase, a quantitative understanding of their most elementary features is still missing. IVR and VET in halogenated hydrocarbons,<sup>1–6</sup> benzene,<sup>7</sup> nitromethane,<sup>8</sup> acetonitrile,<sup>9,10</sup> alcohols,<sup>11–13</sup> and water<sup>14</sup> have been studied in considerable detail in the time domain employing different techniques of (state-selective) pump-and-probe spectroscopy. However, because almost all of the above (and other previous) experiments studied the relaxation in the fundamentals, not much is known about IVR and

VET at higher internal energies or their systematic structure, mode, and solvent dependence.<sup>15–17</sup> Moreover, because intramolecular and intermolecular vibrational energy relaxation are often studied only for one particular molecule, generalizable mechanisms and principles, such as those known for isolated molecules, have not been clearly identified yet. As a consequence, it appears nearly impossible to predict time scales and mechanisms of IVR and VET of molecules in solution or to calculate relaxation rates with sufficient accuracy for both processes.<sup>18,19</sup>

Recently, we have measured intra- and intermolecular relaxation in solution for several molecules of different size and structure.<sup>16,17</sup> One of the major motivations for our studies has been to understand the relationship between the molecules' chemical structure and the rates of IVR and VET, in particular, the rates of intramolecular vibrational energy redistribution. Progress in an understanding of these trends may help to design molecules in which IVR rates in solution can be controlled by

\* To whom correspondence should be addressed. BABEL@GWDG.DE.

<sup>†</sup> Institut für Physikalische Chemie der Universität Göttingen.

<sup>‡</sup> Max-Planck Institut für Biophysikalische Chemie.

(temporary) chemical modification. In this communication, we report real-time measurements of intramolecular vibrational energy redistribution and intermolecular vibrational energy transfer in solution for two alkyl iodides,  $\text{CF}_3\text{CH}_2\text{I}$  and  $\text{CH}_3\text{CH}_2\text{I}$ . The goal of this study is to elucidate the effect of chemical substitution on these processes, that is, replacing three hydrogen atoms by three fluorine atoms and leaving the degrees of freedom, the number of atoms, the excitation energy of the solute, and the solvent unchanged. This study is to some extent similar in spirit to recent experiments in the frequency domain for isolated molecules.<sup>20,21</sup>

## II. Experimental Approach and Setup

In two recent articles, we have given a detailed description of the ideas and concepts of our experimental approach.<sup>16,17</sup> The technique has been employed first very recently by Crim and co-workers to measure the relaxation of  $\text{CH}_2\text{I}_2$  in organic solvents.<sup>3,15</sup> In the meantime, it has been further developed in Crim's and our group to measure IVR and VET in fundamentals, in overtones, and in combination bands of several molecules containing C–I bonds.<sup>3,15–17</sup> Briefly, for the selective excitation and probing of molecules in solution in our experiments, we employ femtosecond (fs) IR-pump and UV-probe transient absorption spectroscopy. A special feature of the experiment is that near-IR laser pulses are used to selectively excite molecules in overtones of C–H stretch vibrations and excited-state populations are monitored by transient UV-absorption spectroscopy. In particular, the vibrational overtone excitation initially prepares some zeroth-order bright state (with vanishing Franck–Condon (FC) factors for the electronic probe transition) corresponding to the first overtone of the C–H (anti) symmetric stretch vibration ( $\nu_{\text{CH}} = 2$ ). The probe laser follows the excitation laser pulse and is tuned to the red wing of the electronic absorption of the molecule in the near-UV spectral range. Because the initially excited “state” is a nonstationary state of the molecular Hamiltonian of the molecule, it evolves in time and vibrational energy flows from the C–H bond to other degrees of freedom including the FC-active modes (for the electronic transition), which were not excited initially. Resonance Raman experiments help to identify such modes. Corresponding experiments on iodides in the gas and liquid phase show that the dominant mode in the Raman spectra of alkyl iodides is the C–I stretch vibration.<sup>22–24</sup> We have found that if all zeroth-order states of the molecule are grouped in tiers (starting with the bright state) FC-active modes appear in the late tiers (“bath”) nearly at the end of the relaxation cascade. Their increasing population enhances the absorption of a time-delayed probe pulse tuned to the long wavelength wing of the electronic absorption spectrum. At the same time, vibrational energy transfer to the solvent takes place and in turn decreases the absorption. By varying the time delay between the vibrational overtone excitation and the UV-probe laser, we can directly measure the times for intramolecular vibrational energy redistribution and for the transfer of vibrational energy to the solvent.<sup>15–17</sup> The characteristics of the corresponding signals are a fast nearly exponential increase of the absorption and a (nearly exponential) decrease of the absorption on a much longer time scale. Another special feature of our experiment is that we convert transient absorption into internal energy using high-temperature absorption spectra measured in shock waves. Although, we detect transient absorption for various probe wavelengths (optimization of  $\lambda_{\text{probe}}$ ), only one probe wavelength and calibration is sufficient in this experiment to probe the internal energy of the molecules.

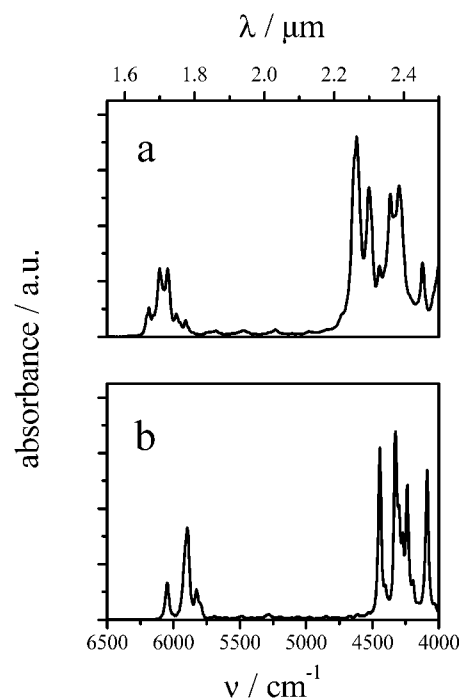


**Figure 1.** Near-IR absorption spectrum of (a)  $\text{CH}_3\text{CH}_2\text{I}$  in  $\text{CCl}_4$  ( $\lambda_{\text{exc}} = 1715 \text{ nm}$ ) and (b)  $\text{CF}_3\text{CH}_2\text{I}$  in  $\text{CCl}_4$  ( $\lambda_{\text{exc}} = 1695 \text{ nm}$ ).

The laser pulses for the pump-and-probe experiment are generated from a home-built regeneratively amplified Ti:sapphire laser system, which has only been described in part in two recent publications.<sup>16,17</sup> While the main part of the output of our Ti:sapphire/RGA system (pulse width  $\sim 50 \text{ fs}$ ) at  $800 \text{ nm}$  is used to pump the optical parametric amplifier (TOPAS, Light Conversion), which generated the near-IR laser pulses close to  $1.7 \mu\text{m}$  used in the experiments (pulse width  $\sim 50 \text{ fs}$ , bandwidth  $\sim 300 \text{ cm}^{-1}$  at  $\lambda_{\text{pump}} = 1700 \text{ nm}$ ), the remaining light of the RGA pumped a home-built widely tunable noncollinear optical parametric amplifier ( $\Delta t \approx 30 \text{ fs}$ ,  $\Delta \nu \approx 300 \text{ cm}^{-1}$ ,  $\lambda_{\text{probe}} \approx 330 \text{ nm}$ ). The excitation and delayed probe pulses are focused ( $f = 200 \text{ mm}$ ) and overlapped with perpendicular polarization in a thin ( $500 \mu\text{m}$ ) quartz flow cell containing the liquid sample ( $1\text{--}2 \text{ M}$  solutions). A concentration dependence of the signals (in the range  $0.5\text{--}3 \text{ M}$ ) has not been observed. During the experiments, laser pulse intensities were properly attenuated to avoid any nonlinear effects. The relatively weak transient difference absorptions in the range  $50\text{--}500 \mu\text{OD}$  ( $\text{OD} = \text{optical density}$ ) in the maximum of the signals were measured at  $1 \text{ kHz}$  with a noise level (after sufficient averaging) of about  $5\text{--}10 \mu\text{OD}$ . For more details, see refs 16 and 17. High-temperature spectra of  $\text{CH}_3\text{CH}_2\text{I}$  and  $\text{CF}_3\text{CH}_2\text{I}$  for the determination of the temperature dependence of the absorption coefficient  $\epsilon(T)$  at selected probe wavelengths, used in our experiments for the conversion of absorption into energies, have been measured in our shock tube setup, which is described elsewhere.<sup>17</sup>

## III. Results and Discussion

In the present set of experiments, we focused on the effect of chemical substitution on the mechanisms and time scales of IVR and VET for two differently substituted hydrocarbons in solution ( $\text{CCl}_4$ ). Near-infrared femtosecond laser pulses at  $1.7 \mu\text{m}$  tuned to the corresponding spectral absorption features in Figure 1 selectively excited  $\text{CF}_3\text{CH}_2\text{I}$  and  $\text{CH}_3\text{CH}_2\text{I}$  in the two-quanta overtone region of the CH stretch vibration in solution.

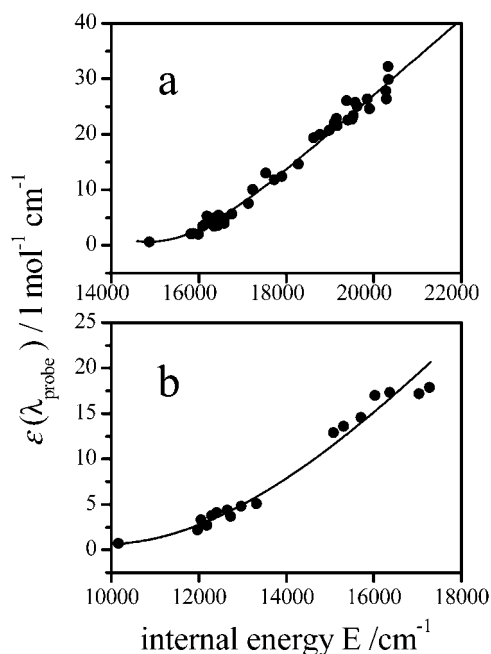


**Figure 2.** Absorption coefficient  $\epsilon$  of (a)  $\text{CH}_3\text{CH}_2\text{I}$  (gas phase) as a function of internal energy  $E$  ( $E$  includes a zero-point energy of  $14\,557\text{ cm}^{-1}$ ) for  $\lambda_{\text{probe}} = 335\text{ nm}$  measured in a shock tube experiment and (b)  $\text{CF}_3\text{CH}_2\text{I}$  as a function of internal energy  $E$  for  $\lambda_{\text{probe}} = 340\text{ nm}$  ( $E$  includes a zero point energy of  $9448\text{ cm}^{-1}$ ). The solid line is a polynomial fit to represent the data: (a)  $\epsilon/(\text{l mol}^{-1}\text{ cm}^{-1}) = 9.304\,29 \times 10^{-15} E^4 - 7.684\,66 \times 10^{-10} E^3 + 2.373\,04 \times 10^{-5} E^2 - 0.317\,962 E + 1553.26$ ; (b)  $\epsilon/(\text{l mol}^{-1}\text{ cm}^{-1}) = 64.04 - 0.014\,58 E + 9.966 \times 10^{-7} E^2 - 1.727 \times 10^{-11} E^3$ .

To convert absorption into energy profiles, the transient absorption was calibrated against high-temperature absorption spectra measured in separate shock-wave experiments. Figure 2 displays the “absorption coefficient”,  $\epsilon$ , of  $\text{CH}_3\text{CH}_2\text{I}$  and  $\text{CF}_3\text{CH}_2\text{I}$  as a function of internal energy,  $E$  (including zero-point energy), for  $\lambda_{\text{probe}} = 335$  and  $\lambda_{\text{probe}} = 340\text{ nm}$ , respectively. The time-delayed rise and subsequent decay of the transient absorption in the UV spectral range at 335 and 340 nm, induced by the IR-pump, monitored IVR and VET for both molecules on a picosecond (ps) time scale. To extract rate constants for IVR and VET, we adopt the simple model introduced in refs 16 and 17. We, in turn, assume a first-order energy decay process of an energy  $E_{\text{loc}}$ , which is “localized” in the initial excitation (i.e., a wave packet that resembles the zeroth-order bright state) to background states. The sum of the energies of the background states we termed “redistributed” energy,  $E_{\text{red}}$ . The intramolecular vibrational energy redistribution process is followed by a significantly slower transfer of vibrational energy to the solvent. For the VET process, we also assume a simple first-order decay. The justification for such a simple model is given in refs 16 and 17. The time dependence of  $E_{\text{red}}$  (our observable in the experiment) is then given by

$$E_{\text{red}} = E_0 \left[ \frac{1/\tau_{\text{IVR}}}{1/\tau_{\text{IVR}} - 1/\tau_{\text{VET}}} \right] (\exp(-t/\tau_{\text{VET}}) - \exp(-t/\tau_{\text{IVR}})) \quad (1)$$

where  $\tau_{\text{IVR}}$  and  $\tau_{\text{VET}}$  are global phenomenological IVR and VET constants and  $E_0$  is the initial excitation energy (excess energies of  $5900$  and  $5831\text{ cm}^{-1}$  with respect to the initial thermal energy) of the solute molecules calculated from the photon energy  $E_0 = h\nu_{\text{IR}}$ . Note that  $E_0$  is not a free parameter in this case.<sup>16,17</sup> Such a model has been found to describe the rise and the decay of the transients well. In this case,  $\tau_{\text{IVR}}$  and  $\tau_{\text{VET}}$  are

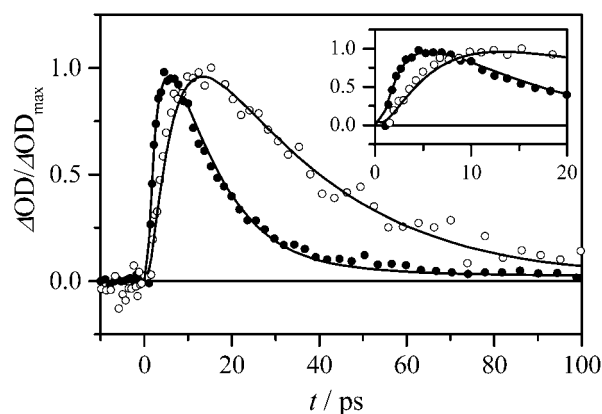


**Figure 3.** Normalized transient absorption time profiles ( $\Delta\text{OD}/\Delta\text{OD}_{\text{max}}$  as a function of delay time) for  $\text{CH}_3\text{CH}_2\text{I}$  (●) and  $\text{CF}_3\text{CH}_2\text{I}$  (○) in  $\text{CCl}_4$  for  $1715\text{ nm}$  and  $1695\text{ nm}$  excitation, respectively. Also shown is a fit using the model described in the text (—). The inset shows the same traces on a shorter time scale.

**TABLE 1: Calculated Normal-Mode Frequencies (B3LYP/6-311G) of  $\text{CH}_3\text{CH}_2\text{I}$  and  $\text{CF}_3\text{CH}_2\text{I}$  (Gas Phase) and Their Symmetry**

mode	$\text{C}_2\text{H}_5\text{I}$		$\text{CF}_3\text{CH}_2\text{I}$	
	symmetry	energy ( $\text{cm}^{-1}$ )	symmetry	energy ( $\text{cm}^{-1}$ )
$\nu_1$	$a''$	3190	$a''$	3228
$\nu_2$	$a''$	3138	$a'$	3162
$\nu_3$	$a'$	3128	$a'$	1525
$\nu_4$	$a'$	3110	$a''$	1366
$\nu_5$	$a'$	3044	$a'$	1306
$\nu_6$	$a'$	1565	$a'$	1270
$\nu_7$	$a''$	1552	$a'$	1180
$\nu_8$	$a'$	1530	$a''$	1107
$\nu_9$	$a'$	1467	$a''$	861
$\nu_{10}$	$a''$	1297	$a'$	826
$\nu_{11}$	$a'$	1271	$a'$	661
$\nu_{12}$	$a'$	1070	$a'$	591
$\nu_{13}$	$a''$	1023	$a''$	505
$\nu_{14}$	$a'$	976	$a'$	488 <sup>a</sup>
$\nu_{15}$	$a''$	763	$a''$	332
$\nu_{16}$	$a'$	492 <sup>a</sup>	$a'$	271
$\nu_{17}$	$a''$	251	$a'$	136
$\nu_{18}$	$a'$	250	$a''$	81

<sup>a</sup> C–I stretch (FC-active).

**TABLE 2: Relaxation Coefficients  $\tau_{\text{IVR}}$  and  $\tau_{\text{VET}}$  for Different Molecules Excited in  $\nu_{\text{CH}} = 2$  in  $\text{CCl}_4$  as Determined from the Simple Model Described in the Text and Number of Low-Order Interactions of the C–H Stretch ( $\nu_{\text{CH}} = 2$ ) to States in the First Tiers**

	$\tau_{\text{IVR}}$ (ps)	$\tau_{\text{VET}}$ (ps)	number of low-order resonances <sup>a</sup>			
			2nd order	3rd order	4th order	5th order
$\text{CH}_3\text{CH}_2\text{I}$	$1.5 \pm 0.5$	$20 \pm 2$	3	6	41	93
$\text{CF}_3\text{CH}_2\text{I}$	$3.5 \pm 0.5$	$50 \pm 5$	1	2	48	305
$\text{CH}_2\text{I}_2^b$	$10 \pm 1$	$70 \pm 8$	1	1	4	19

<sup>a</sup> Number of states in a  $\pm 100\text{ cm}^{-1}$  region around the two-quanta region of the C–H stretch ( $\nu_{\text{CH}} = 2$ ). <sup>b</sup> Charvat, A.; Assmann, J.; Abel, B.; Schwarzer, D. *J. Phys. Chem. A* **2001**, *105*, 5071.

adjustable parameters. This model and  $\epsilon(E)$  were used to fit the experimental traces in Figure 3 (for details, see refs 16 and 17) and to determine overall time constants for the intramolecular vibrational energy equilibration and intermolecular energy transfer for both molecules. The quality of the fits leaves little uncertainty in the determination of the global rate constants summarized in Table 2. While for both molecules the overall features of the transients are similar, the corresponding time

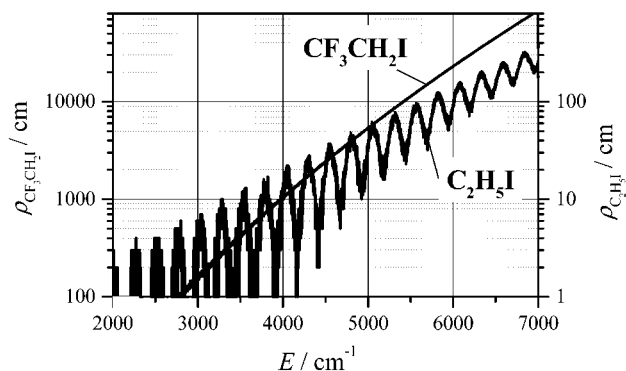


**Figure 4.** Density of states,  $\rho(E)$ , for  $\text{CH}_3\text{CH}_2\text{I}$  and  $\text{CF}_3\text{CH}_2\text{I}$ . Note that the right axis corresponds to  $\rho(\text{CH}_3\text{CH}_2\text{I})$  whereas the left axis corresponds to  $\rho(\text{CF}_3\text{CH}_2\text{I})$ . For more details, see the text.

constants for IVR and VET are markedly different, that is,  $\tau_{\text{IVR}}$  and  $\tau_{\text{VET}}$  are both longer for the fluorinated species. Because the excitation energy and the solvent is the same for both molecules (both having the same structure, number of atoms, and degrees of freedom), the differences in the time scales are directly related to the chemical substitution. Additional studies have shown that these time scales in both cases are hardly affected (or reversed) by the (weakly interacting) solvent. Because fundamentals of both molecules were not available from literature, we have calculated the normal-mode frequencies (gas phase) using density functional theory (DFT) at the B3LYP/6-311G level. These frequencies were used to calculate densities of states,  $\rho(E)$ , for both molecules (using a standard harmonic counting routine), which are displayed in Figure 4. While the state density for  $\text{CF}_3\text{CH}_2\text{I}$  shows an expected fast and smooth increase, the frequency ratio of the normal modes of  $\text{CH}_3\text{CH}_2\text{I}$  is so special that the density of states plot (Figure 4) shows a characteristic “clustering”. Our experimental findings that IVR is significantly faster for the molecule with the significantly lower overall density of states (see Figures 3 and 4) may be surprising at first glance. This observation and other (published and unpublished) experimental results<sup>16,17</sup> provide firm evidence for our conclusion that hierarchical IVR in these molecules “survives” in solution, which is governed by specific low-order intramolecular interactions and which can be rationalized with a simple low-order coupling model.<sup>20,21</sup> In this model, we analyze zeroth-order states of the molecules with approximate harmonic quantum numbers. All zeroth-order states close to the  $\nu_{\text{CH}} = 2$  region in both molecules (in an energy interval  $\pm 100 \text{ cm}^{-1}$ ) have been analyzed with respect to their difference in quantum numbers ( $\sum_i \Delta v_i$  being correlated with the interaction order<sup>20</sup>) and the corresponding energy gap and finally ordered in tiers.<sup>20,21</sup> Different states interact differently with the zeroth-order bright state, with low-order interactions being the strongest. The number of possible low-order resonances for  $\text{CH}_3\text{CH}_2\text{I}$  and  $\text{CF}_3\text{CH}_2\text{I}$ , as well as  $\text{CH}_2\text{I}_2$  (for comparison), is given in Table 2. If we assume that the rate of IVR from the initially excited zeroth-order bright state to the (final) bath of states with energy  $E_{\text{red}}$  is larger for the molecule with the larger number of low(est)-order interactions, the qualitative trends for both molecules and the difference to  $\text{CH}_2\text{I}_2$  can be easily explained! The low-order resonance model employed here is an attempt to explain the overall IVR time constants considering the number of low-order resonances but ignoring the strength of the couplings, which, in the absence of reliable information, are assumed to be all of comparable magnitude. This may be too rough an approximation to explain quantitatively all finer details in the IVR relaxation rates for different molecules and different

excitation energies; however, this is not the aim of the present approach. The development and application of a more sophisticated (quantitative) theoretical model in which IVR is described as a quantum energy flow (diffusion) in quantum number space with a elegant scaling of relevant low-order interactions<sup>25,26</sup> are in progress at present; it actually appears to be able to explain nearly quantitatively all available data from this type of experiment. Results from these studies will be published elsewhere.

While the time scales of VET for both molecules are in the range observed for other molecules,<sup>15–17</sup> the effect of chemical substitution on the rates is rather surprising. We had expected that the introduction of a significant number of low-frequency modes would enhance the rate of VET, because it is commonly believed that the intermolecular vibrational energy transfer is dominated by the low-frequency (or even the lowest-frequency) normal mode(s) in a molecule.<sup>18,19</sup> We have discussed the origin and implications of this viewpoint recently.<sup>16</sup> Upon inspection of the lowest frequencies of the two molecules, we find that the lowest normal-mode frequency in  $\text{CH}_3\text{CH}_2\text{I}$  is about three times larger than that in  $\text{CF}_3\text{CH}_2\text{I}$  (see Table 1). Instead, our present finding is that the  $\text{H} \rightarrow \text{F}$  substitution undoubtedly decelerates the overall VET process in  $\text{CF}_3\text{CH}_2\text{I}$  as opposed to  $\text{CH}_3\text{CH}_2\text{I}$ . The origin of this effect is not completely clear at present. In principle, there are three explanations for this behavior: The first is that IVR in these molecules is not complete such that the lowest frequency modes may not be populated significantly on the time scale of relaxation. Likewise, it may be the case that the lowest frequency modes of both molecules are not very efficient for VET. The third explanation, finally, invokes the different intermolecular pair potentials for hydrogen and fluorine and the corresponding different spectral densities at the corresponding (changed) oscillator frequencies. A further explanation of this effect has to wait for detailed molecular dynamics calculations on these systems, which are underway at present. In addition, investigations of IVR and VET for molecules with other chemical substitutions and structural changes will shed light into these unexpected results.

In conclusion, in this article, we used a mode-specific experimental approach, employing near-infrared and near-ultraviolet femtosecond laser pulses, for the direct measurement of IVR and VET of  $\text{CF}_3\text{CH}_2\text{I}$  and  $\text{CH}_3\text{CH}_2\text{I}$  in  $\text{CCl}_4$ . The changes of the IVR rates upon chemical substitution are somewhat unexpected and provide firm evidence for our conclusion that IVR in these molecules is still governed by specific intramolecular couplings, which survive in solution, and not the overall density of states nor the nature of the weakly interacting solvent. A simple low-order coupling tier model can qualitatively explain the experimental findings. Nevertheless, because of the lack of similar measurements in the gas phase, the absolute impact of the solvent on IVR in the liquid phase is still uncertain. At the same time, the general assumption that VET in solution is always dominated by the lowest-frequency modes in a molecule cannot be supported in this case.

**Acknowledgment.** Financial support from the Deutsche Forschungsgemeinschaft within the SFB 357 (“Molekulare Mechanismen Unimolekularer Prozesse”, A13) and the Fonds der Chemischen Industrie is gratefully acknowledged.

## References and Notes

- (1) Bakker, H. J.; Planken, P. C. M.; Kuipers, L.; Langendijk, A. J. *Chem. Phys.* **1990**, *94*, 1730.



- (2) Bakker, H. J.; Planken, P. C. M.; Langendijk, A. *J. Chem. Phys.* **1991**, *94*, 6007.
- (3) Cheatum, C. M.; Heckscher, M. M.; Bingemann, D.; Crim, F. F. *J. Chem. Phys.* **2001**, *115*, 7086.
- (4) Graener, H.; Lauberau, A. *Appl. Phys. B* **1982**, *29*, 213.
- (5) Graener, H.; Zürl, R. *J. Phys. Chem. B* **1997**, *101*, 1745.
- (6) Hartl, I.; Zinth, W. *J. Phys. Chem. A* **2000**, *104*, 4218.
- (7) Iwaki, L. K.; Deak, J. C.; Rhea, S. T.; Dlott, D. D. *Chem. Phys. Lett.* **1999**, *303*, 176.
- (8) Deak, J.; Iwaki, L. K.; Dlott, D. D. *J. Phys. Chem. A* **1999**, *103*, 971.
- (9) Deak, J. C.; Iwaki, L. K.; Dlott, D. D. *J. Phys. Chem. A* **1998**, *102*, 8193.
- (10) Seifert, G.; Zürl, R.; Graener, H. *J. Phys. Chem. A* **1999**, *103*, 10749.
- (11) Laenen, R.; Rauscher, C. *Chem. Phys. Lett.* **1997**, *274*, 63.
- (12) Laenen, R.; Simeonidis, K. *Chem. Phys. Lett.* **1999**, *299*, 589.
- (13) Lauberau, A.; Kehl, G.; Kaiser, W. *Opt. Commun.* **1974**, *11*, 74.
- (14) Woutersen, S.; Emmerichs, U.; Bakker, H. J. *Science* **1997**, *278*, 658.
- (15) Bingemann, D.; King, A.; Crim, F. F. *J. Chem. Phys.* **2000**, *113*, 5018.
- (16) Charvat, A.; Assmann, J.; Abel, B.; Schwarzer, D. *J. Phys. Chem. A* **2001**, *105*, 5071.
- (17) Charvat, A.; Assmann, J.; Abel, B.; Schwarzer, D.; Henning, K.; Luther, K.; Troe, J. *J. Phys. Chem. Chem. Phys.* **2001**, *3*, 2230.
- (18) Owrutsky, J. C.; Raftery, D.; Hochstrasser, R. M. *Annu. Rev. Phys. Chem.* **1994**, *45*, 519.
- (19) Stratt, R. M.; Maroncelli, M. *J. Phys. Chem.* **1996**, *100*, 12981.
- (20) Nesbitt, D. J.; Field, R. F. *J. Phys. Chem.* **1996**, *100*, 12735.
- (21) Lehmann, K. K.; Scoles, G.; Pate, B. H. *Annu. Rev. Phys. Chem.* **1994**, *45*, 241.
- (22) Phillips, D. L.; Lawrence, B. A.; Valentini, J. J. *J. Phys. Chem.* **1991**, *95*, 7570.
- (23) Phillips, D. L.; Myers, A. B. *J. Chem. Phys.* **1991**, *95*, 226.
- (24) Markel, F.; Myers, A. B. *Chem. Phys. Lett.* **1990**, *167*, 175.
- (25) Schofield, S. A.; Wolynes, P. G. *J. Chem. Phys.* **1992**, *98*, 1123.
- (26) Gruebele, M.; Bigwood, R. *Int. Rev. Phys. Chem.* **1998**, *17*, 91.